ROYAL SOCIETY OF CHEMISTRY

## PAPER

# Synthetic, structural, NMR and catalytic studies of phosphinic amide-phosphoryl chalcogenides (chalcogen = O, S, Se) as mixed-donor bidentate ligands in zinc chemistry†

Miguel A. del Águila-Sánchez,[a] Neidemar M. Santos-Bastos,[b]
Maria C. Ramalho-Freitas,[c] Jesús García López,[a] Marcos Costa de Souza,[b]
Jackson A. L. Camargos-Resende,[c] María Casimiro,[a] Gilberto Alves-Romeiro,[b]
María José Iglesias[a] and Fernando López Ortiz*[a]

*ortho* Substituted (diphenylphosphoryl)-, (diphenylphosphorothioyl)- and (diphenylphosphoroselenoyl)-phosphinic amides $o$-$C_6H_4$(P(X)Ph$_2$)(P(O)N$^i$Pr$_2$) (X = O (**20a**), S (**20b**), Se (**20c**)) were synthesized by *ortho* directed lithiation of $N,N$-diisopropyl-$P,P$-diphenylphosphinic amide (Ph$_2$P(O)N$^i$Pr$_2$) followed by trapping with Ph$_2$PCl and subsequent oxidation of the $o$-(diphenylphosphine)phosphinic amide (**19**) with H$_2$O$_2$, S$_8$ and Se. The reaction of the new mixed-donor bidentate ligands with zinc dichloride afforded the corresponding complexes [ZnCl$_2$(P(X)Ph$_2$)$o$-$C_6H_4$(P(O)N$^i$Pr$_2$)] (**21a–c**). The new compounds were structurally characterized in solution by nuclear magnetic resonance spectroscopy and in the solid-state by X-ray diffraction analysis of the ligand (**20b**) and the three complexes (**21a–c**). The X-ray crystal structure of **20b** suggests the existence of a P=O→P(S)–C intramolecular nonbonded interaction. The natural bond orbital (NBO) analysis using DFT methods showed that the stabilization effect provided by a n$_O$→σ*$_{P–C}$ orbital interaction was negligible. The molecular structure of the complexes consisted of seven-membered chelates formed by O,X-coordination of the ligands to the zinc cation. The metal is four-coordinated by binding to the two chlorine atoms showing a distorted tetrahedral geometry. Applications in catalysis revealed that hemilabile ligands **20a–c** act as significant promoters of the addition of diethylzinc to aldehydes, with **20a** showing the highest activity. Chelation of Et$_2$Zn with **20a** was evidenced by NMR spectroscopy.

## Introduction

Zinc(ɪɪ) compounds are drawing great attention owing to the diversity of applications they show in fields as varied as food additives, electroluminescent and polymeric materials, biological fluorescent probes, *etc.*[1] The inexpensive and environmentally benign nature of zinc makes their complexes attractive catalysts in organic synthesis.[2] Although organophosphorus ligands are ubiquitous in transition metal coordi-

nation chemistry, the use of P=X (X = N, O, S, Se) based ligands for the construction of coordination complexes with zinc dihalides is an area that remains under-explored.

The reaction of neutral monophosphazenes such as MePh$_2$P=NSiMe$_3$ **1** with ZnCl$_2$ furnishes the dimer [ClZn(μ-Cl)-(MePh$_2$P=NSiMe$_3$)]$_2$ in which the monomeric units are connected through μ$_2$-chloro bridges.[3] Functionalised phosphazenes provide access to alternative coordination modes. Thus, the coordinating behaviour of dibenzofuranylphosphazenes **2** (Fig. 1) towards ZnCl$_2$ can be tuned to act as a N-monodentate or N,O-bidentate ligand through the bulkiness of the *N*-aryl substituents giving rise to dimeric (R$^1$ = R$^2$ = Me) and monomeric (R$^1$ = $^i$Pr, R$^2$ = H) complexes, respectively.[4] Bis(phosphazenyl)methane **3**[5] and imine-phosphazene **4**[6] contain two nitrogen atoms in a scaffold that favours the formation of tetracoordinated N,N-chelates with ZnCl$_2$ and ZnI$_2$.

Phosphine oxide ligands coordinate to zinc dihalides to afford complexes with two P=O groups bound to a Zn(ɪɪ) ion with a tetrahedral geometry. The halide atoms occupy the two

[a]*Área de Química Orgánica, Universidad de Almería, Carretera de Sacramento s/n, 04120 Almería, Spain. E-mail: flortiz@ual.es*
[b]*Departamento de Química Orgânica, Universidade Federal Fluminense, Instituto de Química, Rio de Janeiro, Brazil*
[c]*Departamento de Química Inorgânica, Universidade Federal Fluminense, Instituto de Química, Rio de Janeiro, Brazil*

†Electronic supplementary information (ESI) available: NMR spectra of the reported compounds, ORTEP diagrams of **20b** and **21a–c**. CCDC 989179–989182. For ESI and crystallographic data in CIF or other electronic format see DOI: 10.1039/c4dt01789g
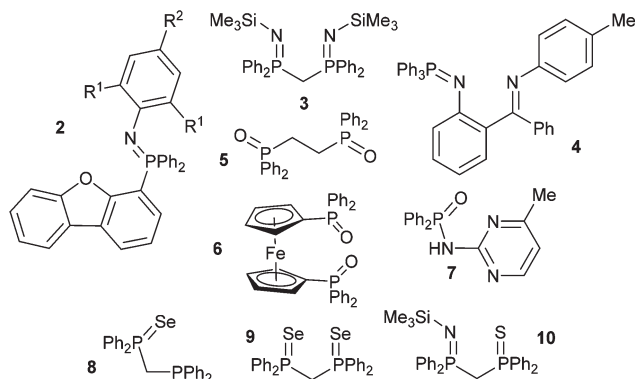
**Fig. 1** Examples of P = X-based bidentate ligands used in the complexation of zinc dihalides.

remaining tetrahedral sites and the architecture of the complexes depends on the spacer connecting the P=O linkages. The simplest structures are obtained by assembling a monodentate triphenylphosphine oxide with $ZnX_2$ (X = Cl, Br, I).[7] The analogous reaction of 1,2-bis(diphenylphosphino ethane)-dioxide **5** (dppeO$_2$) containing two P=O groups linked by an ethylene bridge furnishes 1D polymers $[ZnX_2(\mu\text{-dppeO}_2)]_n$ with alternative dppeO$_2$ and $ZnX_2$ repeating units where the P=O groups exist in an *anti* conformation.[8] In contrast, 1,1′-bis-(diphenylphosphino)ferrocene dioxide **6** (dppfO$_2$) with the P=O groups appended to the more rigid Cp rings of a ferrocenyl system behaves as a chelating ligand in the reaction with $ZnCl_2$ yielding the 1 : 1 adduct $[ZnCl_2(dppfO_2)]$.[9] Interestingly, although the usefulness of the rigid bidentate 1,2-phenylene-bis(diphenylphosphine oxide), $o\text{-C}_6\text{H}_4(\text{P(O)Ph}_2)_2$, as a ligand for the main group, $d^n$ and $f^n$ cations is well-known[10] and the X-ray crystal structure of the free ligand has been described,[11] the complexation behaviour of this ligand with group 12 metals seems to have not been investigated to date.

Zinc complexes of phosphinic amides have been much less studied. Oxygen co-ordination of the P(O)N linkage to metal salts including zinc(II) cations has been proposed based on solution spectroscopic studies and X-ray powder spectra.[12] The only X-ray structure available of a zinc complex with a phosphinic amide ligand is the 1D helical chain formed in the reaction of N-(4-methyl-2-pyrimidinyl)-P,P-diphenyl-phosphinic amide **7** with $ZnCl_2$, $[Zn(7)Cl_2]_n$.[13] In this complex, the ligand bridges the zinc atoms by the coordination of the oxygen atom of the phosphinic amide group and the less hindered nitrogen atom of the pyrimidyl moiety. The two Cl atoms complete the distorted tetrahedral geometry of the zinc cation. Regarding the donor properties of diphenylphosphinic acid derivatives, it has been shown that bis(phosphinic amides) and mixed phosphinic amide-phosphine oxides connected through a trimethylene bridge act as templates for the hydrogen bond-based formation of [2]rotaxanes.[14] The corresponding solid-state structures showed remarkable differences in the hydrogen bond networks. No rotaxane was detected when the corresponding bis(phosphine oxide) was used as a template.

In the same context, zinc co-ordination to softer triorgano-phosphane chalcogenides such as phosphine sulphides and selenides has received scarce attention. Coordination of $ZnCl_2$ and $ZnI_2$ to the sulphur and selenium donor atoms of $Ph_3P=X$, (p-tolyl)$_3$P=X and $(CH_2)_3(Ph_2P=X)_2$ (X = S, Se) has been established by the decrease observed in the IR spectrum of the frequency of the P=X absorption with respect to the free ligand.[15] To the best of our knowledge, only two molecular structures of zinc dihalide complexes have been characterised so far. The (phosphanyl)phosphine selenide **8** and the bis-(phosphine selenide) **9** chelate to $ZnCl_2$[16] and $ZnI_2$,[17] respectively, to give the corresponding metallocycles with a tetrahedral geometry about the zinc cation. Zinc tends to form stable complexes with N- and S-donors, a feature emphasized by the dominance of the $ZnN_2S_2$ structural motif in zinc metalloenzymes and zinc fingers.[18] In line with this, in a study aimed at developing new organozinc catalysts for hydroamination reactions, Roesky and co-workers reported very recently the first examples of zinc complexes of the hybrid P=N/P=S ligand **10** with $ZnCl_2$ and $ZnI_2$.[19]

Williams *et al.* reported the synthesis of *ortho*-(phosphanyl)-phoshinic amides **12** *via* *ortho*-lithiation of phosphinic amides **11** with s-BuLi followed by electrophilic quench with diphenylphosphine chloride (Scheme 1).[20] Compounds **12** proved to be efficient ligands in the palladium catalyzed Suzuki–Miyaura cross-coupling reaction of activated aryl chlorides and strongly deactivated aryl bromides with phenylboronic acid. Moreover, oxidation of **12** with elemental selenium afforded the corresponding (phosphoroselenoyl)phosphinic amides **13**. Recently, we achieved the enantioselective synthesis of **12** *via* *ortho* deprotonation of N-dialkyl-P,P-diphenylphosphinic amides using the complex [n-BuLi·(−)-sparteine] as a base.[21]

As part of our interest in the development of methodologies of *ortho*-lithiations directed by P-based functional groups **14** for accessing bi- and tridentate hemilabile ligands, *e.g.*, **15–17** (Scheme 1),[22] we describe herein the synthesis and structural characterisation of *ortho* substituted (diphenylphosphoryl)-, (diphenylphosphorothioyl)- and (diphenylphosphoroselenoyl)-phosphinic amides, and of their zinc(II) complexes. The difference in the electronic properties between the donor atoms of the polar P=X groups makes these compounds interesting
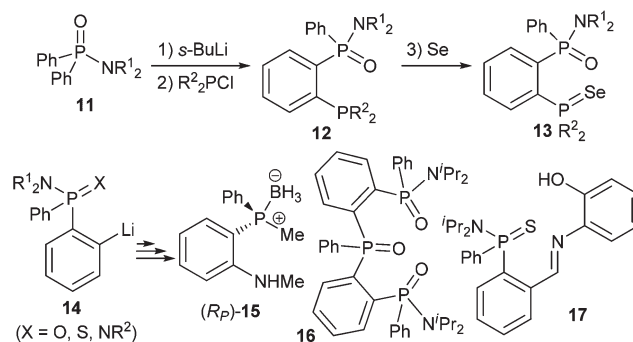


**Scheme 1** Synthesis of P-containing bi- and tri-dentate ligands using directed *ortho* lithiation methods.

ligands for applications in catalysis. Carbon–carbon bond-forming reactions mediated by zinc represent an area of great interest.[2] It can be viewed from two perspectives: zinc salts applied as Lewis acid catalysts and the use of organozinc compounds as reagents for transferring an organic moiety. The results shown here connect both approaches. The potential usefulness of the new ligands has been ascertained by investigating the addition of diethylzinc to aldehydes catalysed by **19** and **20a–c**. No solvent other than the hexane of the Et$_2$Zn solution is used. Ligand **20a** produced a significant enhancement of the rates of formation of ethynylated compounds while minimizing the amount of the reduction by-products generated. The participation of a diethylzinc chelate analogue to the ZnCl$_2$ complexes **21a** as active catalysts is supported by solution NMR measurements.

## Results and discussion

### Synthesis and solution structure of ligands 20 and zinc complexes 21

Bidentate P(O)N/P(X) (X = O; S; Se) ligands **20** were synthesized by *ortho* deprotonation of *N,N*-diisopropyl-*P,P*-diphenylphosphinic amide **18** by treatment with *n*-BuLi in toluene in the presence of *N,N,N′,N′*-tetramethylethylenediamine (TMEDA) at −78 °C. Similar results were obtained when *t*-BuLi in THF was used as a base. The *ortho*-lithium derivative formed was reacted with Ph$_2$PCl to give the *o*-(diphenylphosphanyl)phenyl-phosphinic amide **19**[20,21] in a yield of 85%. Subsequent oxidation of **19** with hydrogen peroxide, elemental sulphur and selenium[20] afforded ligands **20a–c** quantitatively (Scheme 2). The synthesis of ligands **20** can be performed in a one-pot manner by *in situ* oxidation of **19**, albeit in a slightly lower yield (79% for **20a**, 85% for **20b** and 83% for **20c**). Treating ligands **20** with ZnCl$_2$ in a mixture of acetonitrile–dichloromethane (1:1) at room temperature furnished the respective complexes **21** in quantitative yields.

Compound **20c** has been previously synthesized by Williams *et al.*[20] The ESI-HRMS spectra of **20a–b** show the quasimolecular ion peaks [M + H]$^+$ corresponding to the incorporation into **19** of one atom of oxygen (*m/z* 502.2064) and sulphur (*m/z* 518.1838). Concerning complexes **21a–c**, the high

**Table 1** $^{31}$P data of compounds **19–21**, $\delta$ in ppm, $J$ in Hz

| Entry | Comp. | $\delta_{PON}$ | $\delta_{PX}$ | $^3J_{PP}$ |
|---|---|---|---|---|
| 1 | **19** | 33.36 | −10.95 | 6.1 |
| 2 | **20a** | 28.91 | 33.36 | 5.4 |
| 3 | **20b** | 28.11 | 50.07 | 4.5 |
| 4 | **20c** | 27.86 | 41.74 | 4.0$^a$ |
| 5 | **21a** | 37.47 | 41.27 | 8.2 |
| 6 | **21b** | 34.53 | 48.76 | 5.2 |
| 7 | **21c** | 34.15 | 37.24 | 4.3$^b$ |

$^a$ $^1J_{SeP}$ 722 Hz. Reported $^1J_{SeP}$ 718.3 Hz.[20,26] $^b$ $^1J_{SeP}$ 650 Hz.[26]

resolution mass spectra revealed the peaks arising from the loss of one atom of chlorine [M − Cl]$^+$ (**21a** *m/z* 600.0978, **21b** *m/z* 616.0741 and **21c** *m/z* 664.0169). Oxidation of the *ortho* phosphino moiety of **19** is readily ascertained by NMR spectroscopy. Table 1 shows the $^{31}$P NMR data of compounds **20** and **21**. The corresponding NMR parameters of **19** and **20c** have been included for comparison.[20,21] The transformation of the P(III) group of **19** into the P(V) of **20** is evidenced by the large $^{31}$P deshielding, $\Delta\delta_{PX}$(**19–20**) = 44.31 to 61.02 ppm.

The $\delta_{PX}$ values of **20** are in a range typical of phosphine chalcogenides.[23] In contrast, the phosphorus of the phosphinic amide linkage undergoes a small shielding effect with limiting values of $\Delta\delta_{PON}$(**19–20**) = −4.45 and −5.5 ppm, which increases in the series O < S < Se. P(III) oxidation is also accompanied by a decrease in the magnitude of the vicinal $^{31}$P,$^{31}$P coupling constant ($\Delta^3J_{PP}$(**19–20**) = 0.7 to 2.1 Hz).

On complex formations, the infrared spectra of **21** show all the $\nu$(P=X) stretching frequencies to lower values than the parent compounds. The downward shifts are 40–96 cm$^{-1}$ for $\nu$(NP=O),[13] 39 cm$^{-1}$ for $\nu$(P=O),[8] 72 cm$^{-1}$ for $\nu$(P=S)[15] and 5 cm$^{-1}$ for $\nu$(P=Se).[15c] The decrease of $\nu$(P=X) observed is consistent with bidentate coordination of **20** to ZnCl$_2$ either as chelate or bridge ligands.[8,15] The variation of the decrease of $\Delta\nu$(NP=O), in the series **21a** < **21b** < **21c** suggests that P=O interaction of the phosphinic amide linkage with the metal increases with decreasing hardness of the chalcogen of the P=X group.[24] Bidentate binding to zinc is also supported by $^{31}$P NMR spectroscopy. Compared to **20**, the phosphorus atoms of all NP=O moieties appear deshielded (average $\Delta\delta_{PON}$(**21–20**) ≈ 7 ppm), whereas those of the phosphorothioyl and phosphoroselenoyl groups of **21b** and **21c** suffer a shielding of 1.31 and 4.5 ppm, respectively.[24b,25] Regarding the $^{31}$P,$^{31}$P coupling constants, the magnitude is notably greater for **21a** and remains unchanged for **21b,c**. Expectedly, in complex **21c** a significant decrease of the $^{77}$Se,$^{31}$P coupling constant $^1J_{SeP}$ is observed with respect to the free ligand ($\Delta^1J_{SeP}$(**20c–21c**) = 72 Hz) due to the increase of the P=Se bond length upon complex formation.[26] Full assignment of the $^1$H and $^{13}$C NMR spectra of compounds **20** and **21** was achieved based on the analysis of the standard set of $^1$H, $^1$H{$^{31}$P}, $^{13}$C{$^1$H}, dept135, gCOSY45, $^1$H,$^{13}$C-gHSQC, $^1$H,$^{13}$C-gHMBC and $^1$H,$^{31}$P-gHMQC spectra. In addition, 1D gTOCSY, gNOESY and $^{13}$C{$^1$H,$^{31}$P} experiments were performed to complete the structural assignment. A detailed discussion of the
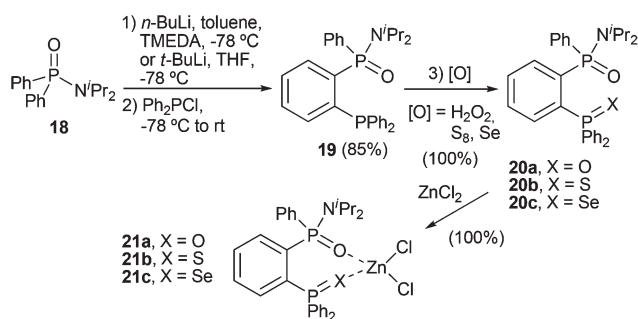


**Scheme 2** Synthesis of *ortho* P=O/P=X (X = O, S, Se) ligands **20** and their zinc(II) complexes **21**.

assignment of the $^1$H and $^{13}$C NMR spectra of complex **21a** is given in the electronic ESI (see Table S1†).

Compounds **21b** and **21c** proved to be poorly soluble in acetone, methanol, acetonitrile and THF. NMR spectra, except $^1$H,$^{13}$C-gHMBC, could be measured in a reasonable spectrometer time from very diluted chloroform solutions. Due to the lack of information about long-range $^1$H,$^{13}$C correlations, some carbons were assigned by their similarity to those of **21a** (see the Experimental section). The analysis of $^1$H and $^{13}$C NMR spectra of **20** and **21** revealed some trends. The principal interest is on the quaternary carbons. They all undergo a shielding on complex formation. The largest decreases of $\delta$ are found for C7 (average $\Delta\delta_{C7}(\textbf{20–21}) \approx 3.9$ ppm), C13 (average $\Delta\delta_{C13}(\textbf{20–21}) \approx 10.2$ ppm) and C19 (average $\Delta\delta_{C19}(\textbf{20–21}) \approx 4.2$ ppm) (Table S1†).

Concerning $^{31}$P,$^{13}$C coupling constants, the greatest changes occur for C1 and C19. In both cases, $^1J_{PC}$ increases in the series **21a** < **21b** < **21c**, with average values ($\Delta^1J_{PC}(\textbf{20–21})$) of −4.4 Hz and −7.4 Hz, respectively. This fact suggests that zinc coordination to the oxygen of the phosphinic amide group shortens the P–C$_{ipso}$ distances and the effect becomes larger the softer the chalcogen of the P=X linkage, *i.e.*, assuming similar geometry of the metallacycles, the tentative indication is that zinc interaction with the oxygen atom of the NP(O) group seems to strengthen when the zinc···X=P interaction weakens.

### Solid-state characterization

Single crystals of ligand **20b** and zinc complexes **21a–c** were obtained by diffusion under an atmosphere of Et$_2$O into dichloromethane–acetonitrile (1:1) solutions of the compounds. The crystal structure of **20b** is shown in Fig. 2, and selected data are summarized in Tables 2 and S2.† The (phosphorothioyl)phosphinic amide **20b** crystallizes in the triclinic space group $P\bar{1}$ together with a molecule of acetonitrile. The solid-state structure is similar to that of bis(diphenylphosphine oxide) o-C$_6$H$_4$(P(O)Ph$_2$)$_2$.[11] The phosphorus atoms are almost coplanar with the *ortho* substituted ring (torsion angle P1–C1–C2–P2 of −5.6(4)°) with the O1 and S1 oriented to the



**Fig. 2** Molecular structure of **20b** (depicted with 50% probability ellipsoids) including atom labels relevant to the structural discussion (see text) and solvent of crystallisation.

**Table 2** Selected bond lengths (Å) and angles (°) for **20b**

| | | | |
|---|---|---|---|
| P1–O1 | 1.473(2) | O1–P1–C1 | 108.2(1) |
| P1–N1 | 1.648(3) | O1–P1–C19 | 114.5(1) |
| P1–C1 | 1.838(3) | N1–P1–C1 | 109.1(1) |
| P1–C19 | 1.802(3) | S1–P2–C2 | 116.7(1) |
| P2–S1 | 1.951(1) | S1–P2–C7 | 108.9(1) |
| P2–C2 | 1.847(3) | S1–P2–C13 | 115.9(1) |
| P2–C7 | 1.827(3) | O1–P1–C1–C2 | −36.6(3) |
| P2–C13 | 1.813(3) | P1–C1–C2–P2 | −5.6(4) |
| O1–P1–N1 | 113.1(1) | S1–P2–C2–C1 | −49.8(3) |

*ortho*-space and allocated in opposite faces out of the plane defined by the *ortho*-phenyl ring (torsion angles O1–P1–C1–C2 and S1–P2–C2–C1 of −36.6(3)° and −49.8(3)°, respectively).[27] The O1 atom lies in anti with respect to a P2-phenyl ring (O1···P2–C7 angle of 169.5(1)°) and the non-covalent separation O1···P2 (3.179 Å) is 0.141 Å shorter than the sum of van der Waals (vdW) radii of the corresponding atoms (3.32 Å). This proximity may be indicative of a weak donor–acceptor intramolecular interaction from a lone pair on O1 into a σ* orbital of the P–C7 bond. This effect would be absent for S1···P1. The separation of 3.693 Å is above the sum of S and P vdW radii (3.6 Å). In order to gain insight into a possible O1···P2–C7 intramolecular hypervalent interaction, DFT calculations at the M06-2X/6-311+G(d,p) level of theory and their NBO analysis[28] were carried out. The results show that the $n_{O1}{\rightarrow}\sigma^*_{P2-C7}$ orbital interaction provides a stabilization of only 0.73 kcal mol$^{-1}$, too weak (<2kT) to be of significance for conformational lock in a thermally fluctuating environment at room temperature.[29] The elongation of P2–C7 as compared with P2–C13 is explained by the difference in the orbital interactions between the S lone pairs with the corresponding antibonding orbitals (stabilization of 16.84/13.88 kcal mol$^{-1}$ for $\sigma^*_{P2-C7}/\sigma^*_{P2-C13}$).[30]

The O1···P2 contact does not seem to produce a noticeable distortion of the expected tetrahedral geometry of P1 and P2, except for a slight increase of the phosphorus-to-carbon bond length of the carbon atom anti to O1 (distance P2–C7 1.827(3) Å) as compared with P2–C13 (1.813(3) Å). The bond angles of P1 and P2 are in the appropriate range for a sp$^3$ hybridization: 114.5(1)°–104.8(1)° for P1 and 116.7(1)°–104.1(1)° for P2. Bond distances in the P=S linkage and the N–P=O moiety are unremarkable (Table 3), with values close to the average distances reported for phosphine sulphides[31] (1.97 Å) and analogue phosphinic amides [P–N (1.662 Å) and P–O (1.484 Å)].[21,22b,32]

The X-ray crystallographic study of complexes **21a–c** revealed that they are monomers which crystallize in the monoclinic space group ($P2_1/c$). The molecular structures are presented in Fig. 3. Selected crystal data and bond lengths and angles are given in Tables S2 and 3.† In compounds **21a–c**, the zinc atom is bonded to the chelating ligands **20a–c** through the chalcogen atom of the P=X linkage (X = O, S, Se) and the oxygen atom of the phosphinic amide group. The seven-membered metallacycles thus formed adopt a twist-boat conformation in which the zinc atom is at the center of a distorted tetrahedron defined by the X,O heteroatoms of the ligands and
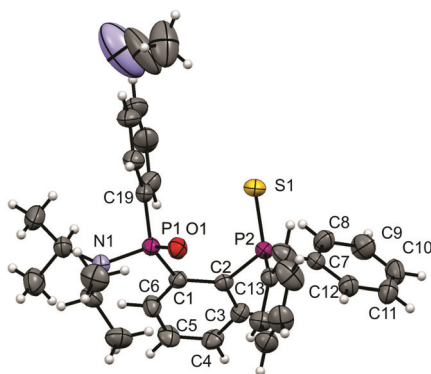
**Table 3** Selected bond lengths (Å) and angles (°) for complexes **21a–c**

| 21a | | 21b | | 21c | |
|---|---|---|---|---|---|
| P1–O1 | 1.496(3) | P1–O1 | 1.495(2) | P1–O1 | 1.497(3) |
| P1–N1 | 1.647(3) | P1–N1 | 1.641(2) | P1–N1 | 1.647(4) |
| P1–C1 | 1.831(4) | P1–C1 | 1.833(2) | P1–C1 | 1.833(4) |
| P1–C19 | 1.792(4) | P1–C19 | 1.796(2) | P1–C19 | 1.798(5) |
| P2–O2 | 1.504(3) | P2–S1 | 1.9987(9) | P2–Se1 | 2.158(1) |
| P2–C2 | 1.832(4) | P2–C2 | 1.828(2) | P2–C2 | 1.833(4) |
| P2–C7 | 1.801(3) | P2–C7 | 1.821(3) | P2–C7 | 1.831(5) |
| P2–C13 | 1.794(4) | P2–C13 | 1.799(2) | P2–C13 | 1.793(5) |
| Zn1–O1 | 1.972(3) | Zn1–O1 | 1.967(2) | Zn1–O1 | 1.975(3) |
| Zn1–O2 | 1.977(2) | Zn1–S1 | 2.3620(7) | Zn1–Se1 | 2.4638(9) |
| Zn1–Cl1 | 2.215(1) | Zn1–Cl1 | 2.2188(7) | Zn1–Cl1 | 2.224(1) |
| Zn1–Cl2 | 2.202(1) | Zn1–Cl2 | 2.2220(8) | Zn1–Cl2 | 2.230(2) |
| Zn1–O1–P1 | 159.1(2) | Zn1–O1–P1 | 166.4(1) | Zn1–O1–P1 | 166.6(2) |
| Zn1–O2–P2 | 129.9(1) | Zn1–S1–P2 | 104.21(3) | Zn1–Se1–P2 | 99.88(4) |
| O2–Zn1–O1 | 90.4(1) | S1–Zn1–O1 | 94.29(5) | O1–Zn1–Se1 | 93.83(9) |



(a)



(b)



(c)
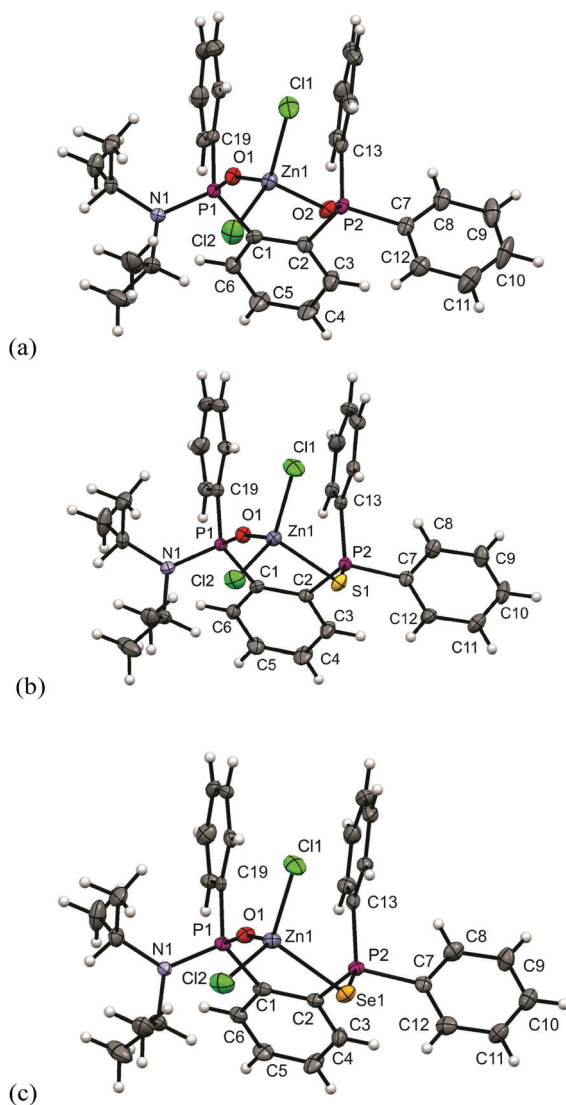
**Fig. 3** Crystal structures of **21a** (a), **21b** (b) and **21c** (c) (depicted with 50% probability ellipsoids) including atom labels relevant to the structural discussion (see text).

the two chlorine atoms. Bonding parameters in complexes **21a–c** are similar to those of the structurally analogue compounds. Chelation produces a slight increase of the P=O/P=X bond distances (P1–O1 range 1.495(2)–1.497(3) Å; P2–O2 1.504(3) Å; P2–S1 1.9987(9) Å; P2–Se1 2.158(1) Å) with respect to the free ligand (Table 3), as observed in related phosphinic amide[13,22c,33] and phosphoryl chalcogenide complexes (chalcogen = O,[7–11] S[31d,34] and Se[16,17,26,31d,35]).[24b] However, it is worth mentioning that the Zn1–S1 bond distance (2.3620(7) Å) observed in **21b** is significantly shorter than that found in [ZnX₂(Ph₂P=NSiMe₃)(Ph₂P=S)CH₂}] (X = Cl, I, average 2.4141 Å).[19] Interestingly, P1–C1 and P1–C19 bond distances are shorter in the complexes than in the free ligands, with P1–C19 being the most affected. These features support the observed increase of $^1J_{PC}$ for C1 and C19 in the $^{13}$C-NMR spectra on complex formation.

Major differences among the structures of complexes **21a–c** are concerned with the geometry of the metallacycle. Bond angles around Zn vary in the range 90.4(1)°–114.92(8)° for **21a**, 94.29(5)°–115.26(5)° for **21b** and 93.83(9)°–115.8(1)° for **21c**, with the bite angle O1–Zn1–Xn of the ligand in **21a** (Xn = O2, 90.4(1)°) being lower than that in **21b** (Xn = S1, 94.29(5)°) and **21c** (Xn = Se1, 93.83(9)°). These values are similar to the bite angle found in the five-membered ring of the complex [ZnCl₂(Ph₂P=Se)CH₂(Ph₂P)], (Se–Zn–P2 94.78(5)°),[16] which illustrates the level of twisting occurring in the metallacycle framework of **21a–c**. Bite angles notably larger than those of **21a–c** are observed in the related complexes [HgX₂(Ph₂P=S)-CH₂CH₂(Ph₂P=S)], (S–Zn–S for X = I[34a] 118.85(8)° and X = Cl[36] 122.3(1)°) and formed between ZnCl₂ and [ZnCl₂(dppfO₂)], (O–Zn–O 102.07(15)°).[9] The more flexible ligand in the former compound and the larger ring size in the latter allows for a better adaptation of the metallacycle to the steric requirements of the molecule. Bite angles close to those of **21a–c** have been found in the complex of 1,2-phenylenebis(diphenylphosphine oxide) with LiOH, [Li(o-C₆H₄(Ph₂P=O)₂)₂]⁺OH⁻, where two ligands chelate a tetrahedral lithium cation with O–Li–O angles of 96.1(6)° and 98.6(6)°.[37] The changes in the bite angle in the series **21a** < **21b** ≈ **21c** also affect other bond angles. For instance, Cl1–Zn1–Cl2 and Cl2–Zn1–O2 are larger in **21a** than in **21b–21c** (Table S3†).

Similar to the free ligand **20b**, the phosphorus atoms of **21a–c** are almost coplanar with the ortho phenyl ring (range of torsion angles P1–C1–C2–P2 −5.9(5)° to −4.7(6)°). The phosphinic amide fragment shows essentially the same pattern in the three complexes (range of torsion angles O1–P1–C1–C2 of −23.5(4)° to −21.9(4)°) with the bulky N$^i$Pr₂ substituent in a pseudo-equatorial position and the pseudo-axial P-phenyl ring oriented almost parallel to one of the phenyl substituents of the Ph₂P=X moiety. This latter group is rotated counter-clockwise around the P2–C2 bond with respect to the plane of the P1–O1 bond and the degree of rotation increases by increasing the size of the chalcogenide. This is clearly seen in the variation of the dihedral angle O1–P1···P2–Xn in the series **21a** (X = O2, 24.9(1)°) < **21b** (X = S1, 32.19(8)°) < **21c** (X = Se1, 33.9(1)°) (see also O2–P2–C2–C1, Table S3†). The phenyl rings

of the Ph$_2$P=X group move accordingly as shown by the increase of the dihedral angles C3–C2–P2–C7 (from 0.0(4)° in **21a** to 11.3(2)° in **21b** and 11.8(4)° in **21c**) and C19–P1···P2–C13 (**21a** 12.1(2)°, **21b** 17.5(1)° and **21c** 18.1(2)°). This rotation of the Ph$_2$P=X group brings the pseudo-equatorial phenyl ring closer to a right angle with H3, thus supporting the view of the increasing shielding of H3 observed in the $^1$H-NMR spectra of **21a–c** as originated by ring current effects (Table S2†).
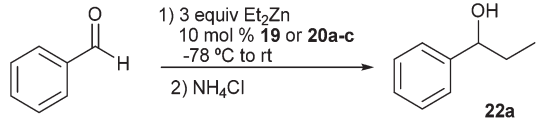
The extent of the twist in the metallacycle is determined by the relative position that the Zn atom adopts. This is characterised by the dihedral angles C1–P1–O1–Zn1 and C2–P2–O2–Zn1. Both become more negative in the series **21a** < **21b** < **21c** (Table S3†). The twist around the zinc atom causes an almost linear arrangement of the metal with the P1–O1 bond (bond angles P1–O1–Zn1 in the range 159.2(2)°–166.6(2)°) and a significant variation of the bond angle P2–Xn–Zn1 from almost trigonal in **21a** (X = O2, 129.9(1)°), to approximately tetrahedral in **21b** (X = S1, 104.21(3)°) and **21c** (X = Se1, 99.88(4)°). For comparison, the P–O–Zn bond angles in the complex [ZnCl$_2$(dppfO$_2$)] containing a larger metallacycle are 158.8(2) and 142.9(2).[9]

### Et$_2$Zn catalyzed addition studies

Having ascertained the feasibility of phosphinic amide-phosphoryl chalcogenides **20** to act as mixed bidentate ligands towards zinc dichloride, we undertook a study of their behaviour as catalysts in a reaction in which O,X-chelation of zinc may promote a rate acceleration. It has been recently shown that the use of *o*-C$_6$H$_4$(P(O)Ph$_2$)$_2$ in the catalytic asymmetric addition of allyl cyanide to ketones[38] and the Mukaiyama aldol reaction with ketones[37] produces a significant acceleration of the reaction rate. Both transformations take place in the presence of alkaline metal phenolates. The activation induced by the bis(phosphine) oxide ligand was assigned to enhanced Lewis basicity of the phenolate by the formation of chelates with alkaline cations based on NMR[38] and X-ray diffraction studies.[37] Other P-based compounds such as 3,3′-diphosphoryl-BINOLs and bifunctional chiral phosphinic amides are very efficient ligands in the highly enantioselective addition of organozinc reagents to aldehydes and ketones.[39]

The phosphinic amide-phosphoryl chalcogenides **20a–c** are hemilabile ligands structurally similar to the bis(diphenylphosphine oxide) *o*-C$_6$H$_4$(P(O)Ph$_2$)$_2$ and the chiral phosphinic amides mentioned above. They provide the opportunity of checking the effect of the mixed donor sites in catalysis. Moreover, they are *P*-stereogenic compounds that can be synthesized in enantiomerically pure form *via* desymmetrization of Ph$_2$P moieties.[21,22h] As a proof of concept, we have investigated the addition of diethylzinc to benzaldehyde in the presence of substoichiometric amount of ligands **20a–c** to give **22a** (Table 4). For the sake of completeness, the catalytic activity of ligand **19** was also evaluated. A procedure analogue to that reported by Ishihara *et al.* has been applied.[39b] Yields of alcohol **22a** were determined by quantitative NMR techniques using 1,5-cyclooctadiene (COD) as an internal standard (see Fig. S30–S32†).[40] Complex formation was achieved by treating

**Table 4** Ethylation of benzaldehyde with Et$_2$Zn catalyzed by ligands **19** and **20a–c**



| Entry | Ligand | Time (h) | Yield$^a$ (%) |
|---|---|---|---|
| 1 | None | 1 | 3 (10) |
| 2 | **19** | 1 | 28 |
| 3 | **20a** | 1 | 86 |
| 4 | **20b** | 1 | 57 |
| 5 | **20c** | 1 | 59 |
| 6 | None | 1.5 | 4 (14) |
| 7 | **20a** | 1.5 | 99 |
| 8 | **20b** | 1.5 | 73 |

$^a$ Numbers in parenthesis indicate the yield of benzylic alcohol formed.

3 equiv. of Et$_2$Zn (1.0 M solution in hexanes) with 10 mol% of compounds **19** and **20a–c** at −78 °C for 30 min. Then benzaldehyde was added and the reaction was allowed to reach room temperature for 1 h. After aqueous workup, 1-phenylpropan-1-ol **22a** was obtained in a yield of 86% for **20a**, 57% for **20b** and 59% for **20c** (Table 4, entries 3–5). In the absence of a ligand only 3% of alcohol **22a** is formed, together with 10% of benzylic alcohol arising from the reduction of benzaldehyde (entry 1).[41,42] Interestingly, ligand **19** with a phosphine substituent at the *ortho* position of the phosphinic amide proved to be notably less efficient (yield of 28%, entry 2) than the chalcogenophosphoryl derivatives **20a–c**. After some experimentation we found that optimal reaction conditions were achieved when the time of contact between the aldehyde and Et$_2$Zn was increased to 90 min. In this way, alcohol **22a** was obtained quantitatively in the presence of **20a** (entry 7), whereas the yield decreased to 73% when the phosphinothioic amide-phosphine oxide **20b** was used as a catalyst (entry 8, see Fig. S30–32†).

These results indicate that ligands **20a–c** accelerate the addition of diethylzinc to benzaldehyde by a factor of 18–25 and virtually suppresses the carbonyl reduction side reaction. Importantly, the hybrid phosphine oxide-phosphinic amide ligand **20a**, *i.e.*, an O,O-chelating ligand featuring subtle differences between the two oxygen atoms, showed the best performance. It is worth noting that in the reaction with **20c** an equimolecular mixture of **19**:**20a** was formed. This means that, even under the mild reaction conditions used, ligand **20c** undergoes complete deselenation leading to the (phosphanyl)-phosphinic amide **19** that is partially oxidized to **20a** during the workup of the reaction. This side-reaction may be favored by the large excess of Et$_2$Zn used (30 equiv.) with respect to the catalytic amount of ligand employed. The comparison of entries 2 and 5 in Table 4 indicates that deselenation of **20c** is not immediate. The yield of 59% obtained for **22a** can be explained by considering that ligand **20c** is acting as a catalyst during a given period of time. Deselenation of **20c** leads to the

formation of **19**, the least efficient catalyst, so the rate of the reaction decreases notably.

The only solvent used in the synthesis of **22a** is the hexane of the $Et_2Zn$ solution. Even under vigorous stirring, the reactions in the presence of ligands **20** are heterogeneous due to the poor solubility of the phosphinic amide-phosphoryl chalcogenides in this non-polar solvent. The ^{1}H-NMR spectrum of a saturated solution of **20a** in hexanes using a capillary of $CDCl_3$ for lock purposes showed the signals of the ligand after vertically scaling the full spectrum by a factor of 1024 (Fig. S33†).[43] The solubility of **20a** in hexane increases in the presence of $Et_2Zn$ due to complexation. The region of aromatic protons of the ^{1}H-NMR spectrum of a saturated sample of **20a** in a 1.0 M solution of $Et_2Zn$ in hexanes revealed the existence of a single species (vertical scaling factor of 256, Fig. S33†). Accordingly, the ^{31}P{^{1}H}-NMR spectrum consisted of only two signals, a doublet at $\delta$ 35.01 ppm ($^3J_{PP}$ = 7.3 Hz) and a very broad signal at $\delta$ 34.15 ppm assigned to the PO and NP(O) groups, respectively (Fig. S34†). The deshielding undergone by both ^{31}P signals and the increase of $^3J_{PP}$ as compared with **20a** are analogous to the changes in the ^{31}P NMR parameters observed upon formation of **21a**. These features indicate that **20a** acts as a mixed O,O-chelate ligand towards $Et_2Zn$ leading to a complex $Et_2Zn·20a$ similar to **21a**.

With this information in hand, we extended the addition of $Et_2Zn$ catalyzed by **20a** to other aldehydes. The results obtained are given in Table 5. For aromatic aldehydes bearing electron-attracting groups (2,4-dichlorobenzaldehyde and furfuraldehyde) and α,β-unsaturated aldehydes ((E)-cinnamaldehyde), the catalyzed ethylation proceeded smoothly to give the corresponding alcohols **22b–d** in high yields in 60–90 min (entries 2, 3 and 4, Fig. S36, S38 and S40,† respectively). Electron-donating groups in aromatic aldehydes such as in 4-(dimethylamino)benzaldehyde slow down the progress of the reaction. Almost quantitative formation of alcohol **22e** is achieved by increasing the reaction time to 20 h (entry 5, Fig. S42†). The ethylation of aliphatic aldehydes takes place less efficiently. Hydrocinnamaldehyde and cyclohexanecarb-

aldehyde underwent addition of the ethyl group to the carbonyl group in the presence of **20a** leading to the respective alcohols **22f** (41%) and **22g** (58%) in moderate yields even after relatively long reaction times (4.5–24 h, entries 6–7, Fig. S44–S46†). In these reactions, small amounts (12%–13%) of the reduction products of the C=O linkage were also observed. The performance of these reactions, though modest, is clearly superior to the uncatalyzed transformations, particularly in the case of cyclohexanecarbaldehyde where a large amount (34%) of the product of hydride transfer from $Et_2Zn$ was formed.

## Conclusions

We have developed a straightforward synthesis of a new type of mixed bidentate ligands **20a–c** containing phosphinic amide and chalcogenophosphoryl (chalcogen = oxygen, sulphur, selenium) donor sites via directed ortho lithiation methods and of their complexes with zinc dichloride **21a–c**. The new compounds were characterised by nuclear magnetic resonance spectroscopy in solution. The molecular structure of **20b** and all zinc(II) complexes **21a–c** was established by X-ray diffraction analysis. The structure of **20b** revealed a P=O···P=S contact. However, NBO analysis showed a negligible stabilisation energy of 0.73 kcal mol$^{-1}$ for the $n_{O1}{\to}\sigma^*_{P-C7}$ orbital interaction, insignificant for conformational control in solution at room temperature.

Ligands **20a–c** gave rise to seven-membered chelate complexes **21a–c** upon reaction with $ZnCl_2$. Metal coordination takes place between the oxygen of the phosphinic amide and the chalcogen of the ortho $Ph_2P=X$ (X = O, S, Se) substituent. The formation of complexes indicates that compounds **20a–c** having mixed-donor groups have potential significance as hemilabile ligands in coordination chemistry. Applications in catalysis support the feasibility of this hypothesis. Compounds **20a–c** act as potent promoters of the addition of diethylzinc to benzaldehyde. The mixed phosphine oxide-phosphinic amide ligand **20a** proved to be the most efficient activator of the three ligands. The extension of the catalysis to other aldehydes showed that high yields of ethylated products are obtained for aromatic, heteroaromatic and α,β-unsaturated aldehydes at room temperature in the presence of 10 mol% of **20a**. For aliphatic aldehydes, ethylalcohols are formed in 41%–58% yield together with small amounts of alcohol arising from the reduction of the starting aldehyde. Further studies on the applications of the new ligands in coordination chemistry and the zinc salt complexes in catalysis[2] are in progress. They include the extension to other transition metals and the use of P-stereogenic mixed ligands in asymmetric catalysis. Bidentate ligands **20** extend the family of mixed phosphinic amide-phosphine oxide ligands **16** (Scheme 1). The potential applications of this type of ligand might be expanded by tuning the donor properties of the phosphinic amide oxygen through stereoelectronic effects produced by the substituents linked to the nitrogen atom.

**Table 5**  Ethylation of aldehydes with $Et_2Zn$ catalyzed by **20a**



| Entry | $R^1$ | 22 | Time (h) | Yield$^a$ (%) | Blank$^a$ (%) |
|---|---|---|---|---|---|
| 1 | $C_6H_5$ | a | 1.5 | 99 | 4(14) |
| 2 | $2,4\text{-}Cl_2C_6H_3$ | b | 1 | 100 | 9(23) |
| 3 | 2-Furyl | c | 1 | 85 | 20 |
| 4 | $(E)\text{-}C_6H_5CH{=}CH$ | d | 1.5 | 97 | 28(37) |
| 5 | $4\text{-}Me_2NC_6H_4$ | e | 20 | 99 | 8 |
| 6 | $C_6H_5CH_2CH_2$ | f | 4.5 | 41(12) | 6(10) |
| 7 | $C_6H_{11}$ | g | 24 | 58(13) | 38(34) |

$^a$ Numbers in parenthesis indicate the yield of reduction by-product formed.

# Experimental

## Materials and methods

All reactions and manipulations were carried out under a dry $N_2$ gas atmosphere using standard Schlenk procedures. THF was distilled from sodium/benzophenone immediately prior to use. Commercial reagents were distilled prior to their use, except alkyllithiums. TLC was performed on Merck plates with aluminum backing and silica gel 60 $F_{254}$. For column chromatography silica gel 60 (40–63 μm) from Scharlau was used. Phosphinamide **18** was prepared as described previously.[22b]

NMR spectra were measured on a Bruker Avance 300 ($^1$H, 300.13 MHz; $^{13}$C, 75.47 MHz; $^{31}$P, 121.49 MHz) and a Bruker Avance 500 spectrometer equipped with a third radio-frequency channel ($^1$H, 500.13 MHz; $^{13}$C, 125.76 MHz and $^{31}$P, 202.45 MHz) using a 5 mm QNP $^1$H/$^{13}$C/$^{19}$F/$^{31}$P probe and a direct 5 mm TBO $^1$H/$^{31}$P/BB triple probe, respectively. The spectral references used were internal tetramethylsilane for $^1$H and $^{13}$C and external 85% $H_3PO_4$ for $^{31}$P. Infrared spectra were recorded in a Bruker Alpha FTIR spectrophotometer. High resolution mass spectra were recorded on Agilent Technologies LC/MSD TOF and HP 1100 MSD instrument using electrospray ionization. Melting points were recorded on a Büchi B-540 capillary melting point apparatus and are not corrected.

## X-ray crystallography

The crystallographic data for ligand **20b** were collected on an Enraf Nonius Bruker KAPPA CCD diffractometer, using graphite monochromatic MoKα radiation ($\lambda$ = 0.71073 Å) at room temperature. Final unit cell parameters were based on the fitting of all reflection positions using DIRAX.[44] Collected reflections were integrated using the EVALCCD program.[45] Empirical multiscan absorption corrections using equivalent reflections were performed with the SADABS program.[46] Data collection of crystals of complexes **21a** and **21b** was performed on an Agilent Gemini Ultra diffractometer, using graphite monochromatic MoKα radiation at 150 K. Data processing (including integration, scaling and absorption correction) was performed using the CrysAlisPro software.[47] The crystal data of complex **21c** were measured at 100 K on a Bruker Smart 1000 CCD diffractometer with MoKα radiation. The cell refinement and data reduction were performed using the Saint[48] software and empirical multiscan absorption corrections were realized with the SADABS program. The structures were solved using Charge Flipping implemented in Superflip.[49] The least-squares refinements were performed with the SHELXL-2013.[50] All atoms except hydrogen were refined anisotropically. Hydrogen atoms were treated by a constrained refinement. Crystallographic data (excluding structure factors) for compounds **20b** and **21a–c** have been deposited in the Cambridge Crystallographic Data Centre no. CCDC: 989179 (**20b**), 989180 (**21a**), 989181 (**21b**), and 989182 (**21c**).

## Computational methods

Geometry optimization of **20b** was performed with the meta-hybrid density functional M06-2X[51] and a 6-311+G(d,p) basis set. Solvation by chloroform ($CHCl_3$) was taken into account by the SMD solvent model,[52] which was applied to both optimization as well as frequency calculation. This stationary point was characterized as minimum and confirmed by vibrational analysis. Orbital interactions were analyzed by using the natural bond orbital (NBO)[28] method at the M06-2X/6-311+G-(d,p) level using the NBO program (version 3.1)[53] implemented in Gaussian 09. The calculations were performed with Gaussian 09.[54] The 3D structure of molecules was generated using CYLView (http://www.cylview.org).

**Synthesis of phosphinic amide (19).** The synthesis of **19** has been described previously.[20,21] A slightly modified procedure has been used. To a solution of phosphinic amide **18** (0.7 g, 2.31 mmol) in 20 mL of toluene and TMEDA (0.49 mL, 2.54 mmol) a solution of n-BuLi (1.6 mL of a 1.6 M solution in hexane, 2.54 mmol) was added at −78 °C (acetone/$CO_2$). After one hour of metallation, chlorodiphenylphosphine (0.46 g, 2.54 mmol) was added. The reaction was stirred at room temperature for 2 hours and then was poured into ice-water, extracted with dichloromethane (3 × 15 mL), washed with sodium thiosulphate (2 × 15 mL), dried over anhydrous sodium sulphate and evaporated to dryness under vacuum to give a white solid. Purification by column chromatography (AcOEt–hexanes 1 : 3) afforded **19** in a yield of 85%. NMR data are in agreement with those reported in the literature.[20,21] Similar results were obtained when the ortho-lithiation was performed with t-BuLi (1.5 mL of a 1.7 M solution in hexane, 2.54 mmol) in THF as a solvent at −78 °C for 2 h.

## General procedure for the synthesis of o-chalcogenophosphoryl-phosphinic amide mixed ligands (20)

*Method A (stepwise).* To a solution of **19** (0.5 g, 1 mmol) in toluene (15 mL) at −10 °C was added 1.1 mmol of the oxidant (0.12 mL of $H_2O_2$ 30% for **20a**, 35 mg of $S_8$ for **20b**, 87 mg of Se powder for **20c**). The reaction was allowed to warm up to ambient temperature and stirred for 30 min at room temperature for **20a**, 12 h for **20b** and 12 h under reflux for **20c**. The solvent was evaporated (in the case of **20c** the slight excess of unreacted selenium was filtered off) and the product extracted with dichloromethane following standard aqueous workup procedures. The crude reaction mixtures consisted of white solids, whose $^{31}$P-NMR spectra showed that compounds **20a–c** were formed quantitatively. The products were filtered and washed with Et$_2$O providing **20a–c** as white solid that were used further in complexation reactions.

*Method B (one-pot).* To a solution of **19** in toluene (or THF) at −10 °C generated as indicated above (assumed 2.31 mmol) was added *in situ* the oxidant (0.28 mL of $H_2O_2$ 30% for **20a**, 81 mg of $S_8$ for **20b**, 0.2 g of Se powder for **20c**). From hereon, the same procedure as described in method A was applied. Products **20a–c** were purified by column chromatography (ethyl acetate–hexanes 4 : 1). See Table 2 for the numbering scheme used.

**Compound 20a.** Yield 79%. White solid. Mp: 195–196 °C. $^1$H-NMR (CDCl$_3$, 500.13 MHz) $\delta$ 1.05 (d, 6H, $^3J_{HH}$ 6.8 Hz, H26/27), 1.12 (d, 6H, $^3J_{HH}$ 6.8 Hz, H26/27), 3.44 (dh, 2H, $^3J_{HH}$ 6.8,

$^3J_{PH}$ 15.1 Hz, H25), 7.01 (m, 2H, H15), 7.10 (m, 2H, H21), 7.18 (m, 1H, H16), 7.22 (m, 2H, H20), 7.28 (m, 1H, H22), 7.36 (m, 2H, H14), 7.37 (m, 2H, H9), 7.45 (m, 1H, H10), 7.73 (m, 1H, H4), 7.74 (m, 1H, H5), 7.80 (m, 2H, H8), 8.18 (m, 1H, H6), 8.58 (m, 1H, H3). $^{13}$C NMR (CDCl$_3$, 125.76 MHz) $\delta$ 23.10 (d, $^3J_{PC}$ 2.6 Hz, C27/26), 23.42 (d, $^3J_{PC}$ 2.9 Hz, C26/27), 47.66 (d, $^2J_{PC}$ 4.1 Hz, C25), 127.26 (d, $^3J_{PC}$ 12.9 Hz, C15), 127.47 (d, $^3J_{PC}$ 12.4 Hz, C21), 127.50 (d, $^3J_{PC}$ 12.7 Hz, C9), 130.38 (d, $^4J_{PC}$ 2.8 Hz, C22), 130.65 (d, $^4J_{PC}$ 2.8 Hz, C16), 130.69 (dd, $^3J_{PC}$ 11.0, $^4J_{PC}$ 2.6 Hz, C5), 130.83 (d, $^4J_{PC}$ 2.8 Hz, C10), 131.03 (dd, $^3J_{PC}$ 11.0, $^4J_{PC}$ 2.5 Hz, C4), 131.61 (d, $^2J_{PC}$ 10.2 Hz, C14), 132.29 (d, $^2J_{PC}$ 9.7 Hz, C20), 132.42 (d, $^2J_{PC}$ 9.8 Hz, C8), 132.86 (d, $^1J_{PC}$ 123.4 Hz, C19), 134.07 (d, $^1J_{PC}$ 111.4 Hz, C7), 134.22 (t, $^2J_{PC}$ = $^3J_{PC}$ 9.3 Hz, C6), 134.34 (d, $^1J_{PC}$ 111.7 Hz, C13), 136.11 (dd, $^1J_{PC}$ 96.4, $^2J_{PC}$ 12.0 Hz, C2), 137.23 (dd, $^2J_{PC}$ 9.1, $^3J_{PC}$ 10.9 Hz, C3), 138.0 (dd, $^1J_{PC}$ 127.6, $^2J_{PC}$ 9.2 Hz, C1) ppm. $^{31}$P NMR (CDCl$_3$, 121.49 MHz) $\delta$ 28.91 (d, $^3J_{PP}$ 5.4 Hz, NP=O), 33.36 (d, $^3J_{PP}$ 5.4 Hz, P=O) ppm. IR (KBr) $\nu$ 1157 (P=O, s), 1215 (NP=O, s) cm$^{-1}$. HRMS (ESI) calcd for C$_{30}$H$_{34}$NO$_2$P$_2$: 502.2065 (MH$^+$), found: 502.2066.

**Compound 20b.** Yield 85%. White solid. Mp: 177–178 °C. $^1$H-NMR (CDCl$_3$, 500.13 MHz) $\delta$ 1.05 (d, 6H, $^3J_{HH}$ 6.8 Hz, H26/27), 1.13 (d, 6H, $^3J_{HH}$ 6.8 Hz, H27/H26), 3.42 (dh, 2H, $^3J_{HH}$ 6.8, $^3J_{PH}$ 14.9 Hz, H25), 7.13 (m, 2H, H15), 7.2 (m, 2H, H21), 7.23 (m, 1H, H16), 7.26 (m, 2H, H9), 7.34 (m, 1H, H22), 7.36 (m, 1H, H10), 7.38 (m, 2H, H20), 7.57 (m, 1H, H4), 7.58 (m, 2H, H14), 7.7 (m, 1H, H5), 7.71 (m, 2H, H8), 8.18 (bm, 1H, H3), 8.23 (m, 1H, H6) ppm. $^{13}$C NMR (CDCl$_3$, 125.76 MHz) $\delta$ 22.96 (d, $^3J_{PC}$ 2.8 Hz, C27/C26), 23.47 (d, $^3J_{PC}$ 2.6 Hz, C26/C27), 47.65 (d, $^2J_{PC}$ 4.0 Hz, C25), 127.44 (d, $^3J_{PC}$ 12.7 Hz, C15 and C21), 127.56 (d, $^3J_{PC}$ 13.0 Hz, C9), 129.97 (d, $^4J_{PC}$ 3.1 Hz, C16), 130.15 (d, $^4J_{PC}$ 3.1 Hz, C10), 130.22 (dd, $^3J_{PC}$ 11.1, $^4J_{PC}$ 2.9 Hz, C5), 130.7 (d, $^4J_{PC}$ 2.7 Hz, C22), 130.78 (dd, $^3J_{PC}$ 12.5, $^4J_{PC}$ 2.5 Hz, C4), 131.48 (d, $^2J_{PC}$ 10.5 Hz, C14), 131.85 (d, $^2J_{PC}$ 10.6 Hz, C8), 132.65 (d, $^2J_{PC}$ 9.6 Hz, C20), 133.02 (d, $^1J_{PC}$ 122.4 Hz, C19), 134.87 (dd, $^2J_{PC}$ 8.9, $^3J_{PC}$ 9.4 Hz, C6), 135.07 (d, $^1J_{PC}$ 90.3 Hz, C7), 135.7 (d, $^1J_{PC}$ 89.9 Hz, C13), 136.97 (dd, $^2J_{PC}$ 11.1, $^1J_{PC}$ 79.3 Hz, C2), 137.22 (dd, $^2J_{PC}$ 13.4, $^3J_{PC}$ 11.4 Hz, C3), 137.51 (dd, $^2J_{PC}$ 9.1, $^1J_{PC}$ 127.5 Hz, C1) ppm. $^{31}$P NMR (CDCl$_3$, 202.45 MHz) $\delta$ 28.11 (d, $^3J_{PP}$ 4.5 Hz, P=O), 50.07 (d, $^3J_{PP}$ 4.5 Hz, P=S) ppm. IR (KBr) $\nu$ 605 (P=S, s), 1215 (NP=O, s) cm$^{-1}$. HR-MS (ESI) calcd for C$_{30}$H$_{34}$NOP$_2$S: 518.1836 (MH$^+$), found: 518.1838.

### General procedure for the synthesis of complexes (21)

To a solution containing 0.10 mmol of the appropriate ligand **20a–c** in 5 mL of a mixture dichloromethane–acetonitrile (1 : 1) was added 0.10 mmol of ZnCl$_2$ (0.1 mL of a 1.0 M solution in diethyl ether) and the reaction was stirred at room temperature overnight. Then, the solvent was evaporated under reduced pressure affording pale yellow powders. The $^{31}$P-NMR spectra of the solids obtained showed that complexes **21a–c** were formed quantitatively. Crystals suitable for X-ray analysis were obtained by slow vapour diffusion of diethyl ether into a solution containing the complex in dichloromethane–acetonitrile (1 : 1).

**Complex 21a.** Yield after recrystallization 61% (39 mg). White solid. Mp: 285–286 °C. $^1$H NMR $\delta$ (CDCl$_3$, 500.13 MHz) $\delta$ 1.02 (d, 6H, $^3J_{HH}$ 6.8 Hz, H26/27), 1.25 (d, 6H, $^3J_{HH}$ 6.8 Hz, H27/26), 3.56 (dh, 2H, $^3J_{HH}$ 6.8, $^3J_{PH}$ 17.3 Hz, H25), 6.99 (m, 2H, H21), 7.04 (m, 2H, H15), 7.18 (m, 2H, H14), 7.25 (m, 1H, H22), 7.28 (m, 2H, H20), 7.29 (m, 1H, H16), 7.33 (m, 1H, H3), 7.39 (m, 2H, H9), 7.53 (m, 1H, H10), 7.57 (m, 2H, H8), 7.64 (m, 1H, H4), 7.91 (m, 1H, H5), 8.37 (m, 1H, H6) ppm. $^{13}$C NMR (CDCl$_3$, 125.76 MHz) $\delta$ 22.98 (d, $^3J_{PC}$ 1.5 Hz, C26/27), 23.30 (d, $^3J_{PC}$ 2.7 Hz, C27/26), 48.10 (d, $^2J_{PC}$ 4.4 Hz, C25), 126.49 (d, $^1J_{PC}$ 108.1 Hz, C13), 127.88 (d, $^3J_{PC}$ 13.3 Hz, C21), 128.28 (d, $^3J_{PC}$ 13.0 Hz, C15), 128.36 (d, $^1J_{PC}$ 126.7 Hz, C19), 128.65 (d, $^3J_{PC}$ 12.9 Hz, C9), 129.87 (d, $^1J_{PC}$ 115.3 Hz, C7), 131.11 (d, $^2J_{PC}$ 10.6 Hz, C14), 132.02 (dd, $^3J_{PC}$ 12.7, $^4J_{PC}$ 2.7 Hz, C4), 132.15 (d, $^2J_{PC}$ 11.0 Hz, C20), 132.26 (d, $^4J_{PC}$ 2.9 Hz, C22), 132.4 (dd, $^3J_{PC}$ 11.4, $^4J_{PC}$ 2.7 Hz, C5), 132.58 (d, $^4J_{PC}$ 3.1 Hz, C16), 132.66 (d, $^2J_{PC}$ 10.5 Hz, C8), 132.8 (d, $^4J_{PC}$ 2.8 Hz, C10), 133.73 (dd, $^2J_{PC}$ 13.3, $^1J_{PC}$ 97.9 Hz, C2), 135.89 (dd, $^1J_{PC}$ 127.5, $^2J_{PC}$ 9.5 Hz, C1), 136.02 (t, $^2J_{PC}$ = $^3J_{PC}$ 9.7 Hz, C6), 137.71 (dd, $^2J_{PC}$ 11.8, $^3J_{PC}$ 14.7 Hz, C3) ppm. $^{31}$P NMR (CDCl$_3$, 121.49 MHz) $\delta$ 37.47 (d, $^3J_{PP}$ 8.2 Hz, NP=O), 41.27 (d, $^3J_{PP}$ 8.2 Hz, P=O) ppm. IR (KBr) $\nu$ 1118 (P=O, s), 1175 (NP=O, s) cm$^{-1}$. HRMS (ESI) calcd for C$_{30}$H$_{33}$ClNO$_2$P$_2$Zn: 600.0967 (M$^+$ − Cl), found: 600.0978.

**Complex 21b.** Yield after recrystallization 51% (34 mg). White solid. Mp: 273–275 °C, $^1$H-NMR (CDCl$_3$, 500.13 MHz) $\delta$ 1.09 (d, 6H, $^3J_{HH}$ 6.8 Hz, H26/27), 1.28 (d, 6H, $^3J_{HH}$ 6.8 Hz, H27/H26), 3.61 (dh, 2H, $^3J_{HH}$ 6.8, $^3J_{PH}$ 16.1 Hz, H25), 6.98 (m, 2H, H15), 7.21 (m, 2H, H21), 7.27 (m, 1H, H16), 7.30 (m, 1H, H3), 7.36 (m, 2H, H20), 7.42 (m, 4H, H8 and H14), 7.43 (m, 1H, H22), 7.45 (m, 2H, H9), 7.55 (m, 1H, H10), 7.59 (m, 1H, H4), 7.86 (m, 1H, H5), 8.43 (m, 1H, H6) ppm. $^{13}$C NMR (CDCl$_3$, 125.76 MHz) $\delta$ 23.12 (d, $^3J_{PC}$ 2.2 Hz, C26/27), 24.1 (d, $^3J_{PC}$ 2.8 Hz, C27/26), 48.7 (d, $^2J_{PC}$ 3.6 Hz, C25), 124.6 (d, $^1J_{PC}$ 86.0 Hz, C13), 128.16 (d, $^3J_{PC}$ 13.6 Hz, C15), 128.49 (d, $^3J_{PC}$ 13.4 Hz, C21), 128.96 (d, $^1J_{PC}$ 130.9 Hz, C19), 129.02 (d, $^3J_{PC}$ 12.7 Hz, C9), 130.93 (d, $^1J_{PC}$ 90.8 Hz, C7), 131.64 (dd, $^3J_{PC}$ 11.3, $^4J_{PC}$ 2.9 Hz, C5), 132.3 (dd, $^3J_{PC}$ 12.7, $^4J_{PC}$ 3.5 Hz, C4), 132.39 (d, $^4J_{PC}$ 3.1 Hz, C10), 132.41 (d, $^4J_{PC}$ 2.9 Hz, C22), 132.54 (d, $^2J_{PC}$ 11.3 Hz, C8), 132.72 (d, $^2J_{PC}$ 10.7 Hz, C14/C20), 132.75 (d, $^2J_{PC}$ 9.8 Hz, C20/C14), 132.95 (d, $^4J_{PC}$ 3.3 Hz, C16), 135.24 (dd, $^1J_{PC}$ 133.4, $^2J_{PC}$ 9.7 Hz, C1), 135.65 (dd, $^1J_{PC}$ 80.7, $^2J_{PC}$ 12.7 Hz, C2), 137.11 (t, $^2J_{PC}$ = $^3J_{PC}$ 9.7 Hz, C6), 138.04 (t, $^2J_{PC}$ = $^3J_{PC}$ 11.8 Hz, C3) ppm. $^{31}$P NMR (CDCl$_3$, 202.45 MHz) $\delta$ 34.53 (d, $^3J_{PP}$ 5.2 Hz, P=O), 48.76 (d, $^3J_{PP}$ 5.2 Hz, P=S). IR $\nu$ 533 (P=S, s), 1125 (NP=O, s) cm$^{-1}$. HRMS (ESI) calcd for C$_{30}$H$_{33}$ClNOP$_2$SZn: 616.0738 (M$^+$ − Cl), found: 616.0741.

**Complex 21c.** Yield after recrystallization 70% (43 mg). Pale brown solid. Mp: 273–275 °C. $^1$H NMR (CDCl$_3$, 500.13 MHz) $\delta$ 1.09 (d, 6H, $^3J_{HH}$ 6.8 Hz, H26/27), 1.31 (d, 6H, $^3J_{HH}$ 6.8 Hz, H27/H26), 3.60 (dh, 2H, $^3J_{HH}$ 6.8, $^3J_{PH}$ 15.6 Hz, H25), 6.99 (m, 2H, H15), 7.23 (m, 5H, H3, H10 and H21), 7.28 (m, 1H, H16), 7.40 (m, 2H, H14), 7.42 (m, 2H, H20), 7.44 (m, 2H, H9), 7.45 (m, 1H, H22), 7.53 (m, 2H, H8), 7.58 (m, 1H, H4), 7.86 (m, 1H, H5), 8.44 (m, 1H, H6) ppm. $^{13}$C NMR (CDCl$_3$, 125.76 MHz) $\delta$ 23.18 (d, $^3J_{PC}$ 2.7 Hz, C26/27), 24.02 (d, $^3J_{PC}$ 3.1 Hz, C27/26), 48.85 (d, $^2J_{PC}$ 3.4 Hz, C25), 123.23 (d, $^1J_{PC}$ 79.1 Hz, C13), 128.35

(d, $^3J_{PC}$ 13.6 Hz, C15), 128.57 (d, $^3J_{PC}$ 13.6 Hz, C21), 129.06 (d, $^3J_{PC}$ 12.3 Hz, C9), 129.22 (d, $^1J_{PC}$ 132.9 Hz, C19), 130.71 (d, $^1J_{PC}$ 80.7 Hz, C7), 131.13 (d, $^2J_{PC}$ 11.6 Hz, C14/20), 131.62 (dd, $^3J_{PC}$ 12.1, $^4J_{PC}$ 3.6 Hz, C5), 132.33 (dd, $^3J_{PC}$ 12.2, $^4J_{PC}$ 3.0 Hz, C4), 132.34 (d, $^4J_{PC}$ 2.8 Hz, C22), 132.44 (d, $^4J_{PC}$ 3.0 Hz, C10), 132.88 (d, $^2J_{PC}$ 10.8 Hz, C8), 132.97 (d, $^4J_{PC}$ 3.4 Hz, C16), 133.17 (d, $^2J_{PC}$ 9.7 Hz, C20/14), 134.55 (dd, $^2J_{PC}$ 10.9, $^1J_{PC}$ 71.1 Hz, C2), 135.38 (dd, $^2J_{PC}$ 9.3, $^1J_{PC}$ 135.1 Hz, C1) 137.08 (t, $^2J_{PC}$ = $^3J_{PC}$ 9.7 Hz, C6), 137.55 (t, $^2J_{PC}$ = $^3J_{PC}$ 12.0 Hz, C3), ppm. $^{31}P$ NMR (CDCl$_3$, 121.49 MHz) $\delta$ 34.15 (d, $^3J_{PP}$ 4.4 Hz, P=O), 37.24 (d, $^3J_{PP}$ 4.4 Hz, P=Se) ppm; $^1J_{SeP}$ 650 Hz. IR $\nu$ 536 (P=Se, s), 1118 (NP=O, s) cm$^{-1}$. HRMS (ESI) calcd for C$_{30}$H$_{33}$ClNOP$_2$SeZn: 664.0178 (M$^+$ − Cl), found: 664.0169.

### General procedure for the addition of Et$_2$Zn to aldehydes catalyzed by ligands 19 and 20a–c

A procedure similar to that reported by Ishihara and co-workers was used.[39b] A well-dried Schlenk tube was charged with the ligand **19** or **20a–c** (0.05 mmol) under a nitrogen atmosphere and cooled to −78 °C. Et$_2$Zn (1.5 mL of 1.0 M solution in hexanes, 1.5 mmol) was added and the suspension was stirred at −78 °C for 30 min. To this suspension, the aldehyde (0.5 mmol) was added and the reaction mixture was stirred at −78 °C for 10 min. After this, the reaction was allowed to gradually reach room temperature and stirred for 1–24 h (see Table 5). When the reaction was complete (see Table 5), it was quenched with 10 mL of sat. NH$_4$Cl aqueous solution and extracted with dichloromethane (10 mL × 3). The combined organic extracts were dried over Na$_2$SO$_4$ and concentrated in a rotavapor. The reaction yield was determined by $^1H$-NMR spectroscopy by integration of the signals of the final products and the signal at $\delta$ 5.57 corresponding to four olefinic protons of COD (0.06 mL, 0.5 mmol).[39]

The NMR sample for determining the coordination of ligand **20a** to Et$_2$Zn was prepared using half amounts of reagents as compared with laboratory scale reactions under otherwise the same conditions. Saturated solutions of **20a** in hexanes were obtained by adding 0.75 mL of hexanes to a Schlenk charged with 12.5 mg of **20a**. In both cases heterogeneous solutions were obtained. After vigorous stirring for 10 min, 0.5 mL of the supernatant solution were placed into a 5 mm NMR tube containing a homemade capillary of CDCl$_3$ (outer diameter of *ca.* 1.5 mm) for lock purposes. $^1H$-, $^1H\{^{31}P\}$- and $^{31}P$-NMR spectra were acquired at room temperature on a Bruker Avance 500 spectrometer (Fig. S33 and S34†). The $^1H$ NMR spectrum of the complex **20a·Et$_2$Zn** revealed that the amount of ligand present in solution was 5 mg. In this case, the integral of the methylene protons of Et$_2$Zn were used as an internal standard.

## Acknowledgements

## Notes and references

1 (a) M. Mézes, M. Erdélyi and K. Balogh, *Eur. Chem. Bull.*, 2012, **1**, 410–413; (b) V. Nishal, A. Kumar, P. S. Kadyan, D. Singh, R. Srivastava, I. Singh and M. N. Kamalasanan, *J. Electron. Mater.*, 2013, **42**, 973–978; (c) D. V. Aleksanyan, V. A. Kozlov, B. I. Petrov, T. V. Balashova, A. P. Pushkarev, A. O. Dmitrienko, G. K. Fukin, A. V. Cherkasov, M. N. Bochkarev, N. M. Lazarev, Y. A. Bessonova and G. A. Abakumov, *RSC Adv.*, 2013, **3**, 24484–24491; (d) B. Gao, R. Duan, X. Pang, X. Li, Z. Qu, H. Shao, X. Wang and X. Chen, *Dalton Trans.*, 2013, **42**, 16334–16342; (e) R. Petrus and P. Sobota, *Dalton Trans.*, 2013, **42**, 13838–13844; (f) C. Nie, Q. Zhang, H. Ding, B. Huang, X. Wang, X. Zhao, S. Li, H. Zhou, J. Wu and Y. Tian, *Dalton Trans.*, 2014, **43**, 599–608.

2 Reviews: (a) C. A. Wheaton, P. G. Hayes and B. J. Ireland, *Dalton Trans.*, 2009, 4832–4846; (b) S. Das, S. Zhou, D. Addis, S. Enthaler, K. Junge and M. Beller, *Top. Catal.*, 2010, **53**, 979–984; (c) X.-F. Wu, *Chem. – Asian J.*, 2012, **7**, 2502–2509; (d) X.-F. Wu and H. Neumann, *Adv. Synth. Catal.*, 2012, **354**, 3141–3160; (e) S. Enthaler, *ACS Catal.*, 2013, **3**, 150–158.

3 C. Valerio-Cárdenas, M.-A. M. Hernández and J.-M. Grévy, *Dalton Trans.*, 2010, **39**, 6441–6448.

4 C. A. Wheaton, B. J. Ireland and P. G. Hayes, *Z. Anorg. Allg. Chem.*, 2011, **637**, 2111–2119.

5 S. Marks, T. K. Panda and P. W. Roesky, *Dalton Trans.*, 2010, **39**, 7230–7235.

6 C. J. Wallis, I. L. Kraft, B. O'Patrick and P. Mehrkhodavandi, *Dalton Trans.*, 2010, **39**, 541.

7 (a) C. A. Kosky, J.-P. Gayda, J. F. Gibson, S. F. Jones and D. J. Williams, *Inorg. Chem.*, 1982, **21**, 3173–3179; (b) T. S. Lobana, in *The Chemistry of Organophosphorus Compounds*, ed. F. R. Hartley, Wiley, New York, 1992, ch. 5, vol. 2, pp. 409–566; (c) A. Zeller, E. Herdtweck and T. Strassner, *Acta Crystallogr., Sect. E: Struct. Rep. Online*, 2001, **57**, m480–m482; (d) Y. Nie, H. Pritzkow, H. Wadepohl and W. Siebert, *J. Organomet. Chem.*, 2005, **690**, 4531–4536.

8 (a) X. Liu, X.-J. Yang, P. Yang, Y. Liu and B. Wu, *Inorg. Chem. Commun.*, 2009, **12**, 481–483; (b) X.-J. Yang, X. Liu, Y. Liu, Y. Hao and B. Wu, *Polyhedron*, 2010, **29**, 934–940.

9 W. Zhang and T. S. A. Hor, *Dalton Trans.*, 2011, **40**, 10725–10730.

10 (a) A. R. J. Genge, W. Levason and G. Reid, *Inorg. Chim. Acta*, 1999, **288**, 142–149; (b) A. R. J. Genge, N. J. Hill, W. Levason and G. Reid, *J. Chem. Soc., Dalton Trans.*, 2001,

1007–1012; (c) N. J. Hill, W. Levason, M. C. Popham, G. Reid and M. Webster, *Polyhedron*, 2002, **21**, 445–455; (d) M. B. Hursthouse, W. Levason, R. Ratnani and G. Reid, *Polyhedron*, 2004, **23**, 1915–1921; (e) M. B. Hursthouse, W. Levason, R. Ratnani, G. Reid, H. Stainer and M. Webster, *Polyhedron*, 2005, **24**, 121–128; (f) K. Nakamura, Y. Hasegawa, H. Kawai, N. Yasuda, Y. Shozo and Y. Wada, *J. Alloys Compd.*, 2006, **408–412**, 771–775; (g) M. F. Davis, W. Levason, R. Ratnani, G. Reid and M. Webster, *New J. Chem.*, 2006, **30**, 782–790; (h) K. Nakamura, Y. Hasegawa, H. Kawai, N. Yasuda, N. Kanehisa, Y. Kai, T. Nagamura, Y. Shozo and Y. Wada, *J. Phys. Chem. A*, 2007, **111**, 3029–3037.

11  M. F. Davis, W. Levason, G. Reid and M. Webster, *Polyhedron*, 2006, **25**, 930–936.

12  M. W. G. de Bolster and W. L. Groeneveld, *Z. Naturforsch., B: Anorg. Chem. Org. Chem. Biochem. Biophys. Biol.*, 1972, **27**, 759–763.

13  C.-W. Yeh and J.-D. Chen, *Inorg. Chem. Commun.*, 2011, **14**, 1212–1216.

14  R. Ahmed, A. Altieri, D. M. D'Souza, D. A. Leigh, K. M. Mullen, M. Papmeyer, A. M. Z. Slawin, J. K. Y. Wong and J. D. Woollins, *J. Am. Chem. Soc.*, 2011, **133**, 12304–12310.

15  (a) K. C. Malhotra, G. Mehrotra and S. C. Chaudhry, *Indian J. Chem., Sect. A: Inorg., Bio-inorg., Phys., Theor. Anal. Chem.*, 1978, **16**, 905–906; (b) T. S. Lobana, S. S. Sandhu and T. R. Gupta, *J. Indian Chem. Soc.*, 1981, **58**, 80–82; (c) T. S. Lobana, T. R. Gupta and S. S. Sandhu, *Polyhedron*, 1982, **1**, 781–783.

16  P. G. Jones and B. Ahrens, Private communication, 2006, CCDC 615020.

17  T. S. Lobana, R. Hundal and P. Turner, *J. Coord. Chem.*, 2001, **53**, 301–309.

18  H. Vahrenkamp, *Dalton Trans.*, 2007, 4751–4759.

19  M. Kuzdrowska, B. Murugesapandian, L. Hartenstein, M. T. Gamer, N. Arleth, S. Blechert and P. W. Roesky, *Eur. J. Inorg. Chem.*, 2013, 4851–4857.

20  D. B. G. Williams, S. J. Evans, H. de Bod, M. S. Mokhadinyana and T. Hughes, *Synthesis*, 2009, 3106–3112.

21  C. Popovici, P. Oña-Burgos, I. Fernández, L. Roces, S. García-Granda, M. J. Iglesias and F. López-Ortiz, *Org. Lett.*, 2010, **12**, 428–431.

22  (a) J. García-López, I. Fernández, M. Serrano-Ruiz and F. López-Ortiz, *Chem. Commun.*, 2007, 4674–4676; (b) I. Fernández, P. Oña-Burgos, G. Ruiz Gómez, C. Bled, S. García-Granda and F. López-Ortiz, *Synlett*, 2007, 611–614; (c) P. Oña-Burgos, I. Fernández, L. Roces, L. Torre-Fernández, S. García-Granda and F. López-Ortiz, *Organometallics*, 2009, **28**, 1739–1747; (d) J. García-López, V. Yáñez-Rodríguez, L. Roces, S. García-Granda, A. Martínez, A. Guevara-García, G. R. Castro, F. Jiménez-Villacorta, M. J. Iglesias and F. López-Ortiz, *J. Am. Chem. Soc.*, 2010, **132**, 10665–10667; (e) C. Popovici, I. Fernández, P. Oña-Burgos, L. Roces, S. García-Granda and F. López-

Ortiz, *Dalton Trans.*, 2011, **40**, 6691–6703; (f) H. el Hajjouji, E. Belmonte, J. García-López, I. Fernández, M. J. Iglesias, L. Roces, S. García-Granda, A. El Laghdach and F. López-Ortiz, *Org. Biomol. Chem.*, 2012, **10**, 5647–5658; (g) F. J. Sainz-Gonzalo, M. Casimiro, C. Popovici, A. Rodríguez-Diéguez, J. F. Fernández-Sánchez, I. Fernández, F. López-Ortiz and A. Fernández-Gutiérrez, *Dalton Trans.*, 2012, **41**, 6735–6748; (h) M. Casimiro, L. Roces, S. García-Granda, M. J. Iglesias and F. López-Ortiz, *Org. Lett.*, 2013, **15**, 2378–2381; (i) M. Casimiro, J. García-López, M. J. Iglesias and F. López-Ortiz, *Dalton Trans.*, 2014, DOI: 10.1039/c4dt00927d.

23  G. Davidson, in *The Chemistry of Organophosphorus Compounds*, ed. F. R. Hartley, Wiley, New York, 1992, ch. 5, vol. 2, pp. 169–193.

24  (a) N. Burford, *Coord. Chem. Rev.*, 1992, **112**, 1–18; (b) J. B. Cook, B. K. Nicholson and D. W. Smith, *J. Organomet. Chem.*, 2004, **689**, 860–869.

25  S. Ahmad, A. A. Isab, H. P. Perzanowski, M. S. Hussain and M. N. Akhtar, *Transition Met. Chem.*, 2002, **27**, 177–183.

26  Measured from the $^{77}Se$ satellites in the $^{31}P$ NMR spectrum. (a) H. Duddeck, *Progr. NMR Spectrosc.*, 1995, **27**, 1–323; (b) H. Duddeck, *Annu. Rep. NMR Spectrosc.*, 2004, **52**, 105–166; (c) A. Pop, A. Silvestru, M. Concepción-Gimeno, A. Laguna, M. Kulcsar, M. Arca, V. Lippolis and A. Pintus, *Dalton Trans.*, 2011, **40**, 12490–12479.

27  This arrangement is commonly found in sterically constrained 1,8-disubstituted (phosphino)naphthalene dioxides and disulphides: (a) A. Karaçar, M. Freytag, H. Thönnessen, J. Omelanczuk, P. G. Jones, R. Bartsch and R. Schmutzler, *Heteroat. Chem.*, 2001, **12**, 102–113; (b) J. Omelanczuk, A. Karacar, M. Freytag, P. G. Jones, R. Bartsch, M. Mikolajczyk and R. Schmutzler, *Inorg. Chim. Acta*, 2003, **350**, 583–591.

28  (a) A. E. Reed and F. Weinhold, *J. Chem. Phys.*, 1983, **78**, 4066–4073; (b) A. E. Reed, L. A. Curtiss and F. Weinhold, *Chem. Rev.*, 1988, **88**, 899–926.

29  N. E. Jackson, B. M. Savoie, K. L. Kohlstedt, M. Olvera de la Cruz, G. C. Schatz, L. X. Chen and M. A. Ratner, *J. Am. Chem. Soc.*, 2013, **135**, 10475–10483.

30  (a) A. E. Reed and P. V. R. Schleyer, *J. Am. Chem. Soc.*, 1990, **112**, 1434–1435; (b) J. A. Dobado, H. Martínez-García, J. Molina-Molina and M. R. Sundberg, *J. Am. Chem. Soc.*, 1998, **120**, 8461–8471; (c) S. Noury and B. Silvi, *Inorg. Chem.*, 2002, **41**, 2164–2172.

31  (a) W. W. Schweikert and E. A. Meyers, *J. Phys. Chem.*, 1968, **72**, 1561–1565; (b) P. W. Codding and K. A. Kerr, *Acta Crystallogr., Sect. B: Struct. Crystallogr. Cryst. Chem.*, 1978, **34**, 3785–3787; (c) F. R. Knight, A. L. Fuller, A. M. Z. Slawin and J. D. Woollins, *Polyhedron*, 2010, **29**, 1849–1853; (d) F. R. Knight, A. L. Fuller, M. Bühl, A. M. Z. Slawin and J. D. Woollins, *Chem. – Eur. J.*, 2010, **16**, 7617–7634; (e) V. Y. Aleksenko, E. V. Sharova, O. I. Artyushin, D. V. Aleksanyan, Z. S. Klemenkova, Y. V. Nelyubina, P. V. Petrovskii, V. A. Kozlov and I. L. Odinets, *Polyhedron*, 2013, **51**, 168–179.

32 (*a*) Mazhar-Ul-Haque and C. N. Caughlan, *J. Chem. Soc., Perkin Trans. 2*, 1976, 1101–1104; (*b*) F. Cameron and F. D. Duncanson, *Acta Crystallogr., Sect. B: Struct. Crystallogr. Cryst. Chem.*, 1981, **37**, 1604–1608; (*c*) B. Davidowitz, T. A. Modro and M. L. Niven, *Phosphorus Sulfur*, 1985, **22**, 255–263; (*d*) I. Fernández, A. Forcén-Acebal, S. García-Granda and F. López-Ortiz, *J. Org. Chem.*, 2003, **68**, 4472–4485; (*e*) H. De Bod, D. B. G. Williams, A. Roodt and A. Muller, *Acta Crystallogr., Sect. E: Struct. Rep. Online*, 2004, **60**, o1241–o1243.

33 (*a*) L.-C. Liang, W.-Y. Lee, T.-L. Tsai, Y.-L. Hsu and T.-Y. Lee, *Dalton Trans.*, 2010, **39**, 8748–8758; (*b*) B. Bichler, L. F. Veiros, Ö. Öztopcu, M. Puchberger, K. Mereiter, K. Matsubara and K. A. Kirchner, *Organometallics*, 2011, **30**, 5928–5942; (*c*) C. Holzhacker, C. M. Standfest-Hauser, M. Puchberger, K. Mereiter, L. F. Veiros, M. J. Calhorda, M. D. Carvalho, L. P. Ferreira, M. Godinho, F. Hartl and K. Kirchner, *Organometallics*, 2011, **30**, 6587–6601; (*d*) C.-W. Yeh, K.-H. Chang, C.-Y. Hu, W. Hsu and J.-D. Chen, *Polyhedron*, 2012, **31**, 657–664.

34 (*a*) T. S. Lobana, M. K. Sandhu, M. J. Liddell and E. R. T. Tiekink, *J. Chem. Soc., Dalton Trans.*, 1990, 691–694; (*b*) O. Crespo, M. C. Gimeno, P. G. Jones and A. Laguna, *Inorg. Chem.*, 1994, **33**, 6128–6131; (*c*) G. J. Depree, N. D. Childerhouse and B. K. Nicholson, *J. Organomet. Chem.*, 1997, **533**, 143–151; (*d*) A. Karaçar, M. Freytag, H. Thönnessen, J. Omelanczuk, P. G. Jones, R. Bartsch and R. Schmutzler, *Z. Anorg. Allg. Chem.*, 2000, **626**, 2361–2372; (*e*) K. Saikia, B. Deb, B. J. Borah, P. P. Sarmah and D. K. Dutta, *J. Organomet. Chem.*, 2012, **696**, 4293–4297.

35 (*a*) T. S. Lobana, R. A. Castineiras and P. Turner, *Inorg. Chem.*, 2003, **42**, 4731–4737; (*b*) K. J. Kilpin, W. Henderson and B. K. Nicholson, *Dalton Trans.*, 2010, **39**, 1855–1864; (*c*) G. S. Ananthnaga, N. Edukondalua, J. T. Mague and M. S. Balakrishna, *Polyhedron*, 2013, **62**, 203–207.

36 T. S. Lobana, R. Verma, A. Singh, M. Shikha and A. Castineiras, *Polyhedron*, 2002, **21**, 205–209.

37 M. Hatano, E. Takagi and K. Ishihara, *Org. Lett.*, 2007, **9**, 4527–4530.

38 R. Yazaki, N. Kumagai and M. Shibasaki, *J. Am. Chem. Soc.*, 2010, **132**, 5522–5531.

39 (*a*) M. Hatano, T. Miyamoto and K. Ishihara, *Synlett*, 2006, 1762–1764; (*b*) M. Hatano, T. Miyamoto and K. Ishihara, *Org. Lett.*, 2007, **9**, 4535–4538; (*c*) M. Hatano and K. Ishihara, *Chem. Rec.*, 2008, **8**, 143–155; (*d*) M. Hatano, T. Mizuno and K. Ishihara, *Synlett*, 2010, 2024–2028; (*e*) M. Hatano, T. Mizuno and K. Ishihara, *Chem. Commun.*, 2010, **46**, 5443–5445; (*f*) M. Hatano, R. Gouzu, T. Mizuno, H. Abe, T. Yamada and K. Ishihara, *Catal. Sci. Technol.*, 2011, **1**, 1149–1158; (*g*) H. Huang, H. Zong, G. Bian and L. Song, *J. Org. Chem.*, 2012, **77**, 10427–10434; (*h*) B. Shen, H. Huang, G. Bian, H. Zong and L. Song, *Chirality*, 2013, **25**, 561–566; (*i*) H. Zong, H. Huang, G. Bian and L. Song, *Tetrahedron Lett.*, 2013, **54**, 2722–2725.

40 T. R. Hoye, B. M. Eklov and M. Voloshin, *Org. Lett.*, 2004, **6**, 2567–2570.

41 It has been reported that benzaldehyde undergo reduction to benzylalcohol upon treatment with Et$_2$Zn at 0 °C in toluene in the presence of (−)-3-*exo*-(dimethylamino)-isoborneol (equimolecular ratio of reagents). No ethylation was observed. M. Kitamura, S. Suga, K. Kawai and R. Noyori, *J. Am. Chem. Soc*, 1986, **108**, 6071.

42 It has been suggested that reduction of aldehydes and ketones by Et$_2$Zn takes place by β-hydride elimination from the organozinc reagent with release of ethylene. (*a*) G. E. Coates and D. Ridley, *J. Chem. Soc. A*, 1966, 1064–1069; (*b*) G. Arnott and R. Hunter, *Tetrahedron*, 2006, **62**, 992–1000.

43 Strong magnetic susceptibility $\chi$ effects were observed. The residual signal of CHCl$_3$ (of the CDCl$_3$ capillary) appears at $\delta$ 6.7 ppm. The signal of the methylene protons at $\delta$ 1.3 ppm was used as a reference. This value was obtained from the $^1$H NMR spectrum of a sample of the same solvent (hexanes) dissolved in CDCl$_3$ See: I. C. Jones, G. J. Sharman and J. Pidgeon, *Magn. Reson. Chem.*, 2005, **43**, 497. The reference used represents a correction of +0.54 ppm due to differences of $\chi$. This correction was applied to the $^{31}$P NMR spectrum.

44 R. W. W. Hooft, *COLLECT*, Nonius Software, The Netherlands, 1998.

45 A. J. M. Duisenberg, *J. Appl. Crystallogr.*, 1992, **25**, 92–96.

46 G. M. Sheldrick, *SADABS, Program for Empirical Absorption Correction of Area Detector Data*, University of Göttingen, Germany, 1996.

47 *Agilent Technologies, CrysAlisPro Software System, version 1.171.35.21, Xcalibur CCD System*, Agilent Technologies UK Ltd., Oxford, UK, 2011.

48 Siemens Analytical X-ray Instruments Inc., *SAINT: Area-Detector Integration Software*, Siemens Industrial Automation, Inc., Madison, WI, 1995.

49 L. Palatinus and G. Chapuis, *J. Appl. Crystallogr.*, 2007, **40**, 786–790.

50 G. M. Sheldrick, *Acta Crystallogr., Sect. A: Fundam. Crystallogr.*, 2008, **64**, 112–122.

51 Y. Zhao and D. G. Truhlar, *Theor. Chem. Acc.*, 2008, **120**, 215–241.

52 A. V. Marenich, C. J. Cramer and D. G. Truhlar, *J. Phys. Chem. B*, 2009, **113**, 6378–6396.

53 E. D. Glendening, A. E. Reed, J. E. Carpenter and F. Weinhold, NBO Version 3.1. (1 ed.).

54 M. J. Frisch, G. W. Trucks, H. B. Schlegel, G. E. Scuseria, M. A. Robb, J. R. Cheeseman, G. Scalmani, V. Barone, B. Mennucci, G. A. Petersson, H. Nakatsuji, M. Caricato, X. Li, H. P. Hratchian, A. F. Izmaylov, J. Bloino, G. Zheng, J. L. Sonnenberg, M. Hada, M. Ehara, K. Toyota, R. Fukuda, J. Hasegawa, M. Ishida, T. Nakajima, Y. Honda, O. Kitao, H. Nakai, T. Vreven, J. A. Montgomery Jr., J. E. Peralta, F. Ogliaro, M. Bearpark, J. J. Heyd, E. Brothers, K. N. Kudin, V. N. Staroverov, T. Keith, R. Kobayashi, J. Normand, K. Raghavachari, A. Rendell, J. C. Burant, S. S. Iyengar, J. Tomasi, M. Cossi, N. Rega, J. M. Millam,

M. Klene, J. E. Knox, J. B. Cross, V. Bakken, C. Adamo, J. Jaramillo, R. Gomperts, R. E. Stratmann, O. Yazyev, A. J. Austin, R. Cammi, C. Pomelli, J. W. Ochterski, R. L. Martin, K. Morokuma, V. G. Zakrzewski, G. A. Voth, P. Salvador, J. J. Dannenberg, S. Dapprich, A. D. Daniels, O. Farkas, J. B. Foresman, J. V. Ortiz, J. Cioslowski and D. J. Fox, *Gaussian 09, Revision B.01*, Gaussian, Inc., Wallingford, CT, 2010.